10 External validation (AN, SB)

In the absence of any superior-quality source position catalogue, a state-of-the-art CRF does not find a data set to which it can be compared to assess its own quality. However, the results of the estimation process of radio source positions always depend on a simultaneous estimate of the whole suite of unknown parameters in the VLBI model. For this reason, the results of site coordinates and velocities as well as of the Earth orientation parameters belong to a certain CRF determination in a consistent way when estimated together. An external validation of a complete VLBI adjustment and of the CRF results can, thus, be carried out through an indirect quality assessment applied to the TRF and the EOP results alone.

10.1 Earth Orientation Parameters

For a comparison of the full set of EOP results, i.e., polar motion and UT1−UTC and their time derivatives as well as the offsets in the two nutation angles, it has to be noted that only for the polar motion components an external evaluation is possible through GPS providing a suitable data set with the same or even better quality. The official EOP series (igs00p03.erp) of the International GNSS Service (IGS) was used for the following comparisons. After subtracting a bias and a rate the six solutions considered initially for ICRF2 exhibit a level of agreement of roughly 120 μas in both components (Table 11). Figure 23 and Figure 24 depict the behavior of the pole components in the form of medians calculated every seven days for plus/minus 35 days. Noticeable systematic variations seem to be more prominent in the y component which have been identified to belong to changes in the IVS network constellations [Artz et al., 2008]. In general, the scatter of the VLBI results and the systematic network effects are at the same level indicating that the wrms values are representative for the overall agreement.

The other three components of the standard Earth orientation representation, UT1−UTC and nutation in dX and dY, can only be determined by VLBI observations with sufficient accuracy. For these components no suitable external (i.e. non-VLBI) comparison is available. An evaluation can, thus, only be carried out by inter-comparing the results of the six solutions. This is a valid approach here since the six time series have been generated by three different software packages. In order to subtract a common signal for a better interpretation, the IERS 05C04 EOP series has been used as a reference. It should be mentioned that the wrms differences (Table 12) and the graphs do not show any quality in an absolute sense since the 05C04 series for UT1−UTC and nutation is mainly driven by VLBI results, however computed with different inputs and for a different purpose. For this reason, the quality of these EOP components should only be derived by contemplating the level of relative agreement.

Taking these considerations into account, a first criterion of the quality should be any systematic behavior visible in the plots (Figure 25 and Figure 26). It is easily discernible that the four Calc/Solve solutions and the SteelBreeze solution by MAO do not exhibit strong systematic variations in the 70-day-median representation. However, a very obvious effect with an irregular period is visible in the IAA time series. This effect has been caused by errors in the submitted IAA EOP file. Since the MAO and the IAA time series do not show strong correlations but the MAO rather follows the four Calc/Solve solutions with some excess noise, it can be concluded that the numerical results provide a reliable relative indication of the quality of each input series.

In Table 12, the MAO solution agrees with the IERS 05C04 series with

Table 11: wrms differences of the different VLBI solutions w.r.t. IGS

Analysis Center	X Pole Offset [μas]	X Pole Rate [μas/day]	X Pole wrms [μas]	Y Pole Offset [μas]	Y Pole Rate [μas/day]	Y Pole wrms [μas]
BKG	-87.0 $\pm$ 4.3	12.4 $\pm$ 1.7	131.0	-125.1 $\pm$ 4.1	-13.2 $\pm$ 1.6	125.2
GSF	-86.6 $\pm$ 3.7	11.4 $\pm$ 1.5	111.4	-132.3 $\pm$ 3.5	-15.2 $\pm$ 1.4	106.7
MAO	-21.3 $\pm$ 4.3	6.3 $\pm$ 1.7	124.8	-93.9 $\pm$ 4.1	-10.1 $\pm$ 1.5	120.1
IAA	-140.5 $\pm$ 4.1	13.5 $\pm$ 1.6	123.5	-137.3 $\pm$ 3.9	-17.2 $\pm$ 1.5	119.6
OPA	-80.4 $\pm$ 3.7	7.6 $\pm$ 1.5	115.2	-119.1 $\pm$ 3.5	-13.8 $\pm$ 1.4	109.1
USN	-79.1 $\pm$ 4.0	9.0 $\pm$ 1.6	121.3	-141.2 $\pm$ 3.8	-12.9 $\pm$ 1.5	115.7

Table 12: wrms differences of the different VLBI solutions w.r.t. IERS 05C04 for nutation

Analysis Center	Nutation dX Offset [μas]	Nutation dX Rate [μas/day]	Nutation dX wrms [μas]	Nutation dY Offset [μas]	Nutation dY Rate [μas/day]	Nutation dY wrms [μas]
BKG	19.0 $\pm$ 1.9	-2.0 $\pm$ 0.4	76.6	-8.1 $\pm$ 2.2	3.4 $\pm$ 0.5	93.3
GSF	34.7 $\pm$ 1.6	-1.8 $\pm$ 0.3	61.9	19.7 $\pm$ 1.8	3.9 $\pm$ 0.4	75.9
MAO	-14.2 $\pm$ 2.6	-1.2 $\pm$ 0.6	100.5	-31.1 $\pm$ 2.7	2.1 $\pm$ 0.7	107.2
IAA	-6.1 $\pm$ 3.5	-11.2 $\pm$ 0.8	143.8	95.7 $\pm$ 3.5	13.5 $\pm$ 0.9	147.8
OPA	37.1 $\pm$ 1.8	-1.2 $\pm$ 0.4	69.8	24.0 $\pm$ 1.8	-2.1 $\pm$ 0.5	76.3
USN	35.8 $\pm$ 1.9	-2.5 $\pm$ 0.4	76.7	32.6 $\pm$ 2.2	3.3 $\pm$ 0.6	92.9

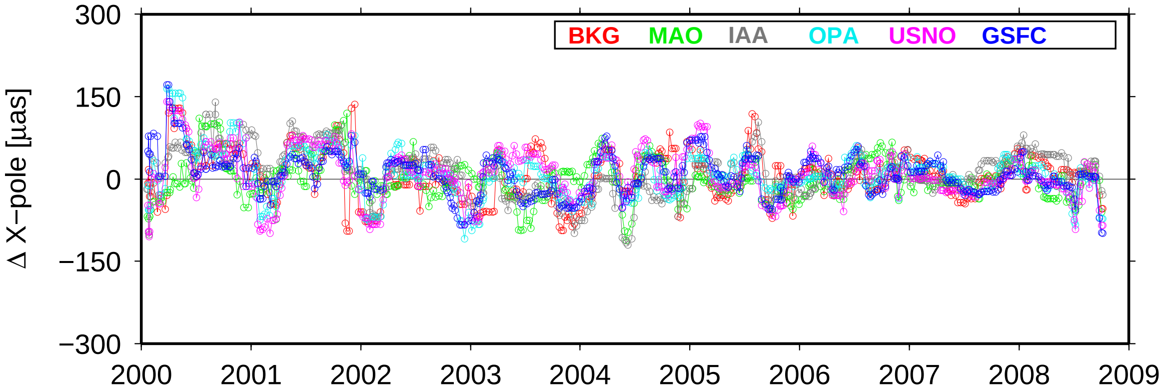

Figure 23: 70-day-median smoothed X pole difference w.r.t. IGS (igs00p03.erp)

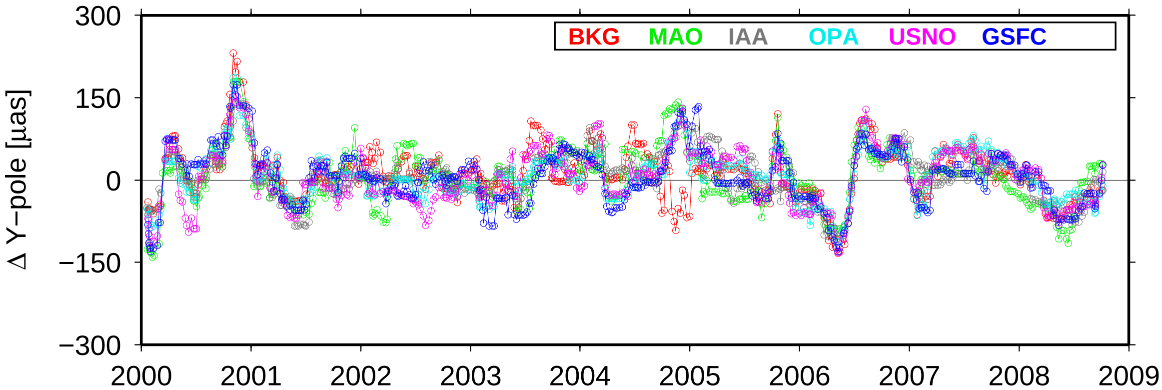

Figure 24: 70-day-median smoothed Y pole difference w.r.t. IGS (igs00p03.erp)

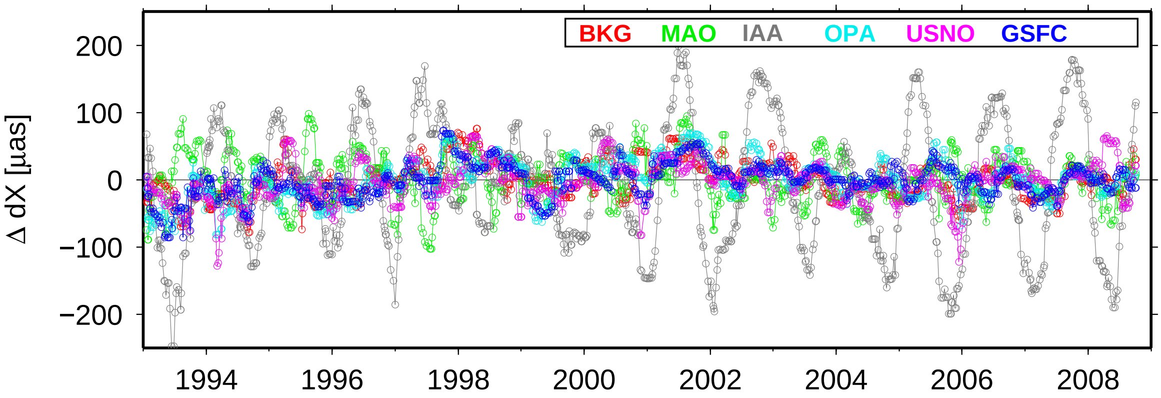

Figure 25: 70-day-median smoothed dX nutation differences w.r.t. IERS 05C04

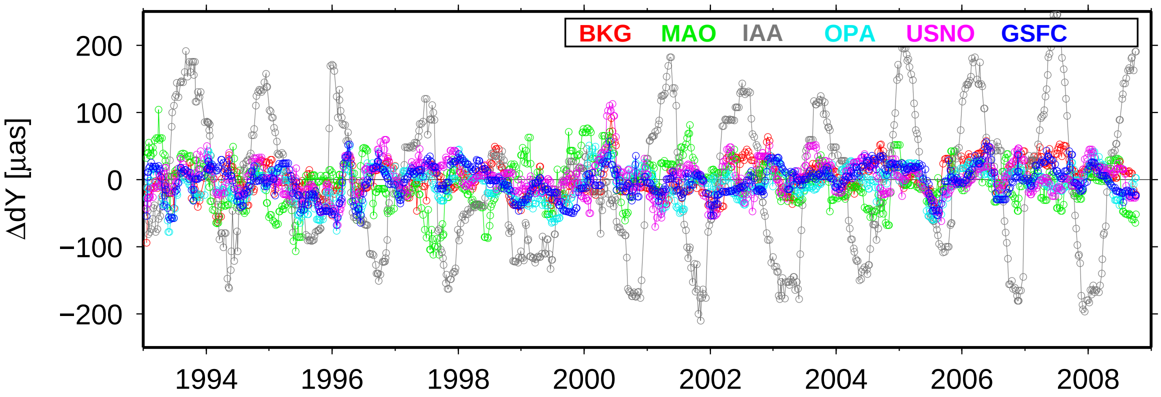

Figure 26: 70-day-median smoothed dY nutation differences w.r.t. IERS 05C04

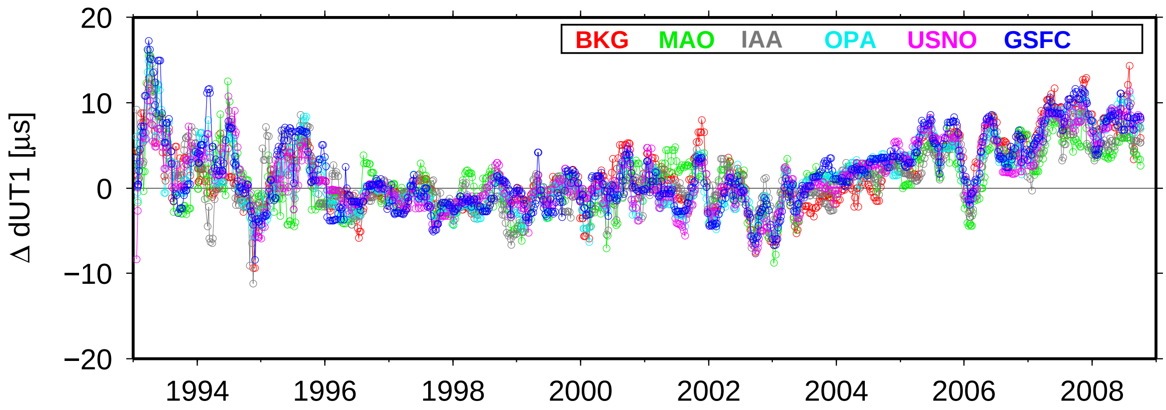

Figure 27: 70-day-median smoothed UT1−UTC differences w.r.t. IERS 05C04

Table 13: wrms differences of the different VLBI solutions w.r.t. IERS 05C04 for UT1−UTC

Analysis Center	UT1−UTC Offset [μs]	Rate [μs/day]	wrms [μs]
BKG	-4.47 ± 0.23	-0.40 ± 0.06	9.08
GSF	-3.88 ± 0.21	-0.38 ± 0.06	8.60
MAO	-0.07 ± 0.24	-0.43 ± 0.07	9.21
IAA	-0.95 ± 0.21	-0.17 ± 0.06	8.56
OPA	-4.10 ± 0.21	-0.21 ± 0.06	8.63
USN	-4.91 ± 0.22	-0.15 ± 0.06	8.77

100 and 107 μas in a wrms sense and the Calc/Solve solutions at the level of 60 to 95 μas. Since these time series all agree with the reference series at a similar level, the absolute accuracy of the nutation estimates should not be worse than by a factor of $\sqrt{2}$. This indicates that the nutation accuracy is at the same level as that of polar motion.

A comparison of the six time series for UT1−UTC shows a slightly different problem (Figure 27). The reference series IERS 05C04 exhibits a long term drift after 2002.5. Nevertheless, the VLBI solutions agree with each other at the few μs level. Table 13 provides the wrms differences w.r.t. the reference series at the level of about 9 μs which corresponds to 135 μas. Obviously, this number is driven by the systematic effect in the differences and does not characterize the agreement of the six series as such. This agreement is rather at the level of 4–5 μs. The level of the agreement of the UT1−UTC results, thus, matches that of the polar motion results and the 100 μas can, therefore, be considered as the upper limit also of this component of Earth rotation.

Biases of the polar motion components of the individual solutions w.r.t. to IERS 05C04 are below 85 μs. The orientations of the terrestrial axes are, thus, effected at the same level.

From the comparisons of the EOP results, it can be concluded that the solutions initially considered for the computation of ICRF2 agree with each other at the level of better than 100 μas excluding obvious systematic deficiencies. The polar motion results of the solution selected for ICRF2, gsf008a, agree with the IGS GPS results by 111 and 107 μas for the x and y component, respectively. Considering that the other EOP components do not exhibit any obvious systematic effects, it can be concluded that their accuracy is at the same level. An upper bound of 110 μas or 3.3 mm at the Earth's surface can thus be inferred for the overall accuracy of each observing session contributing to the determination of ICRF2.

10.2 Terrestrial Reference Frame

A second option for external validations is to investigate what quality the terrestrial reference frame (TRF) has which was estimated in the same process as the CRF was. Since the decision has been made to use the gsf008a solution for ICRF2, the respective TRF has been compared to other TRFs. A comparison of different TRF is most practically being carried out by estimating the parameters of a 14 parameter Helmert transformation and a study of the respective residuals. Ideally, a comparison should be made to the latest realization of the International Terrestrial Reference System, the ITRF2008. Unfortunately, ITRF2008 has not been released at this time. Therefore, VTRF2008 which is the TRF determined from the VLBI input to ITRF2008 is the best independent TRF currently available for this purpose [Böckmann, Nothnagel, & Artz, 2009].

VTRF2008 is a TRF combination product from input of several IVS Analysis Centers and should provide a very reliable reference due to the stabilizing effect of the combination. Seven of nine contributions had been accepted after a detailed quality check excluding two solutions which did not match the high quality criteria. Six of the seven ACs accepted had used the program package Calc/Solve and only one other solution by DGFI was generated with an independent software package, OCCAM. Although it would be better to have more solutions from different software packages, the agreement of all the accepted solutions in general and between the software packages of Calc/Solve and OCCAM in particular should exclude any serious deficiencies in the combined TRF.

The second reference TRF to compare the gsf008a TRF to, is ITRF2005 [Altamimi et al., 2007]. However, ITRF2005 has a known deficiency due to a flaw in the pole tide modeling of the VLBI input. Due to the pole tide error and the unbalanced distribution of observing sites, any comparisons to ITRF2005 will show a noticeable difference in the scale factor [Altamimi et al., 2007; Böckmann et al., 2007].

The Helmert parameters of the gsf008a solution w.r.t. VTRF2008 and ITRF2005 are listed in Table 14. In the context of ICRF2, the rotations and their time evolution are of particular importance. The gsf008a solution is rotated w.r.t. VTRF2008 by not more than 41 μas and w.r.t. ITRF2005 by not more than 3 μas. The rotation rates are at the level of a few μas/yr with formal errors at the same level. The scale difference and its rate w.r.t. VTRF2008 is so small that it is hardly significant. The well known scale effect of ITRF2005 of 0.4 ppb appears as expected.

Table 14: Helmert parameters of TRF(gsf008a) w.r.t. VTRF2008 and ITRF2005

Helmert	VTRF2008		ITRF2005		
Parameter	value	σ	value	σ	unit
T_x	−0.69	±0.36	−0.26	±0.94	mm
T_y	−0.22	±0.35	0.00	±0.87	mm
T_z	−0.21	±0.34	0.11	±0.87	mm
R_x	−31.8	±13.9	0.5	±30.0	μas
R_y	−41.2	±13.2	−0.7	±35.3	μas
R_z	15.2	±9.2	2.9	±32.2	μas
ΔS	−0.006	±0.050	−0.406	±0.138	ppb
T_x/dt	−0.06	±0.09	−0.24	±0.14	mm/y
T_y/dt	0.09	±0.09	0.13	±0.15	mm/y
T_z/dt	0.22	±0.09	0.11	±0.14	mm/y
R_x/dt	−4.61	±3.7	−5.50	±5.96	μas/y
R_y/dt	−2.35	±3.5	−7.57	±5.19	μas/y
R_z/dt	−2.52	±3.2	−1.63	±4.83	μas/y
ΔS/dt	−0.009	±0.014	−0.015	±0.022	ppb/y

The quality of the coordinates and velocities of individual observatories can best be discussed by looking at the post fit residuals of the epoch positions and of the velocities. Observing sites active at the reference epoch of the station positions (2000.0) generally show differences w.r.t. VTRF2008 below 5 mm in the horizontal topocentric positions (Figure 28) with velocities at the 1 mm/y level and below (Figure 29). Notable exceptions are SYOWA and OHIGGINS in Antarctica, TIGOCONC in Chile and NYALES20 on Spitsbergen with horizontal residuals being slightly larger. However, the vertical differences (Figure 30) of these sites fit to VTRF2008 very well. The other stations with larger residuals are older radio telescopes which have been decommissioned already some time ago.

The comparison with ITRF2005 shows a similar picture (Figure 31 and Figure 32). However, a number of sites did have only a short observing history at that time and differences are, thus, larger. In addition, the error in the 2005 VLBI pole tide model appears as a zonal effect in the differences today. For this reason, ITRF2005 turns out not to be a suitable reference for an external validation of the solution for ICRF2 on an individual site basis.

On the basis of the Helmert parameters of the gsf008a TRF estimates w.r.t. the two reference TRFs (VTRF2008 and ITRF2005) it can be stated that the solution fulfills the requirements in terms of the orientation of the axes. The residuals of horizontal and vertical coordinate

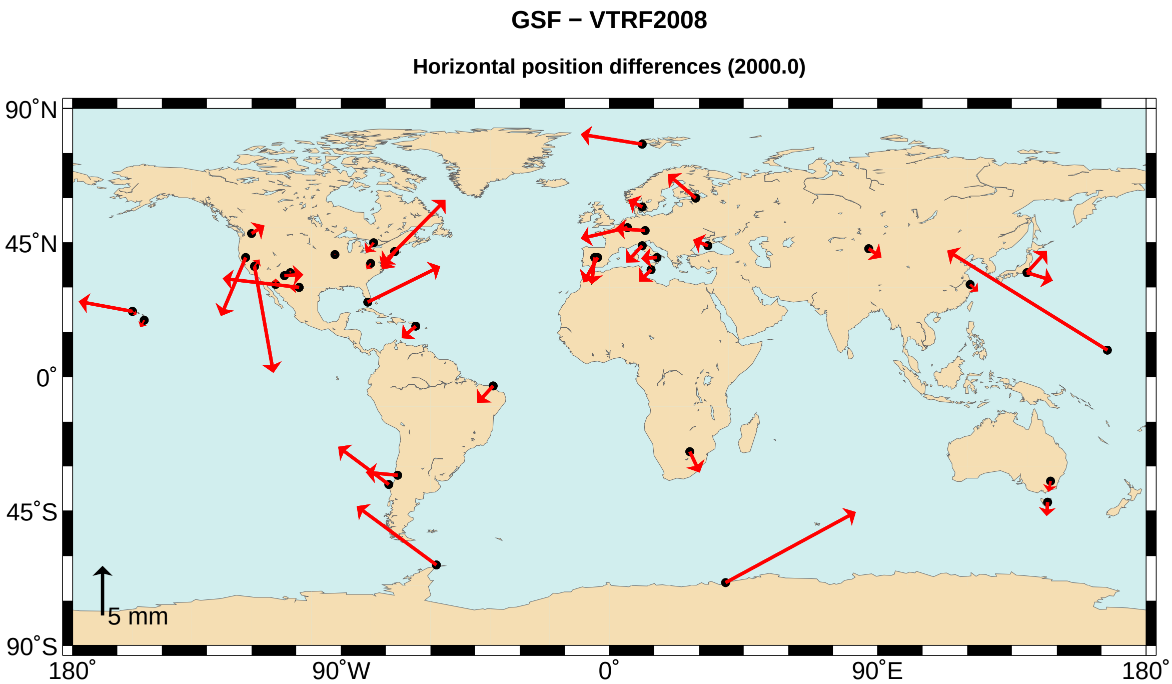

Figure 28: Position differences gsf008a−VTRF2008 at epoch 2000.0

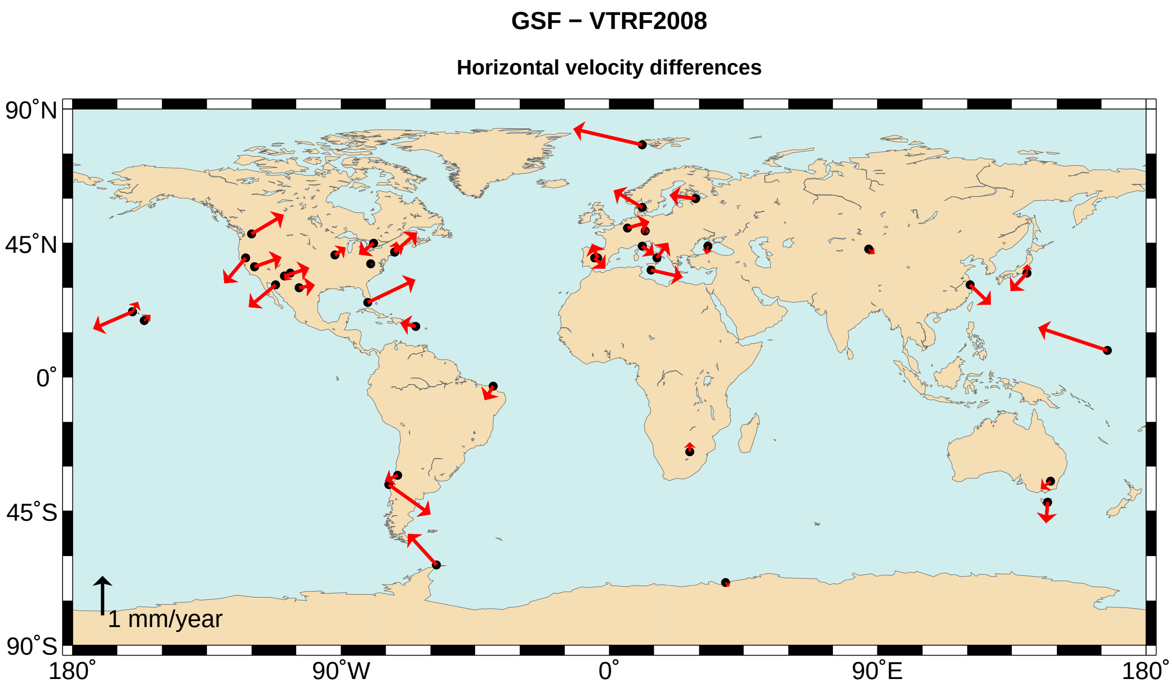

Figure 29: Velocity differences gsf008a−VTRF2008

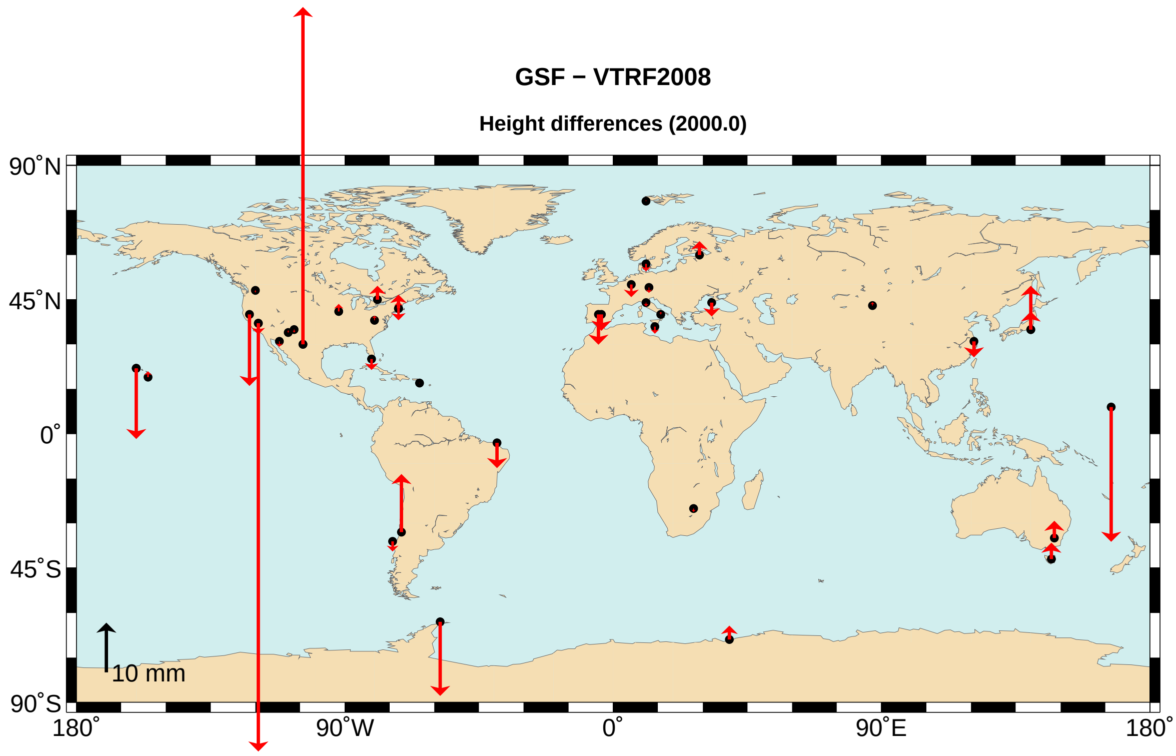

Figure 30: Height differences gsf008a−VTRF2008 at epoch 2000.0

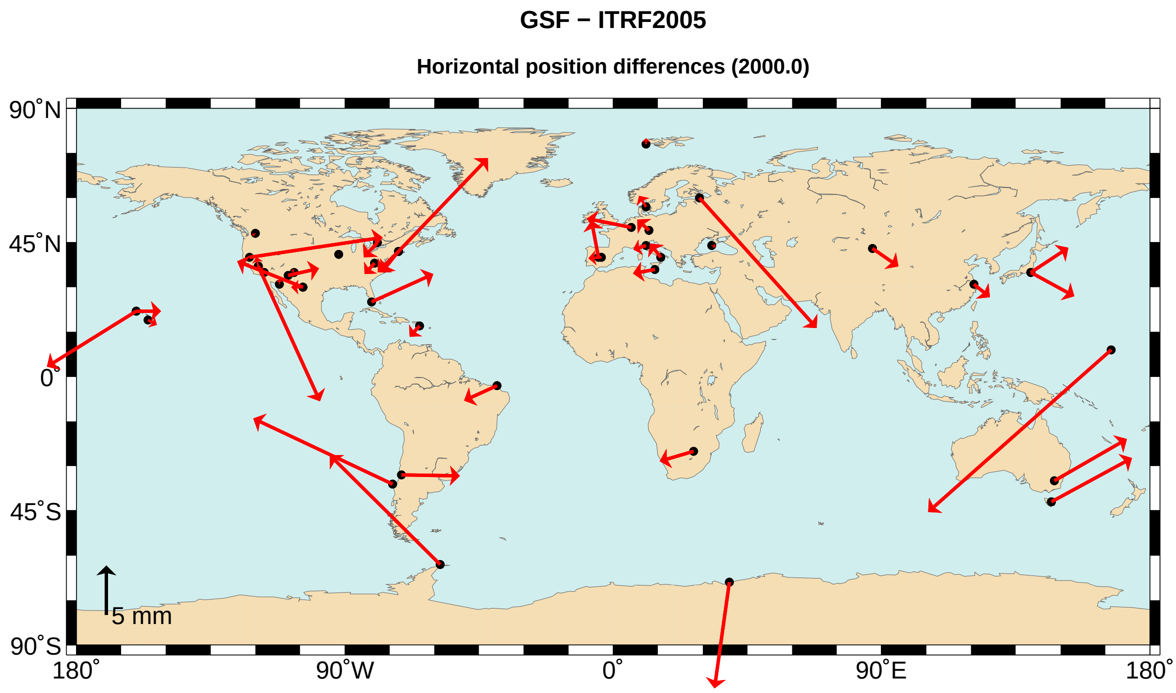

Figure 31: Position differences gsf008a−ITRF2005 at epoch 2000.0

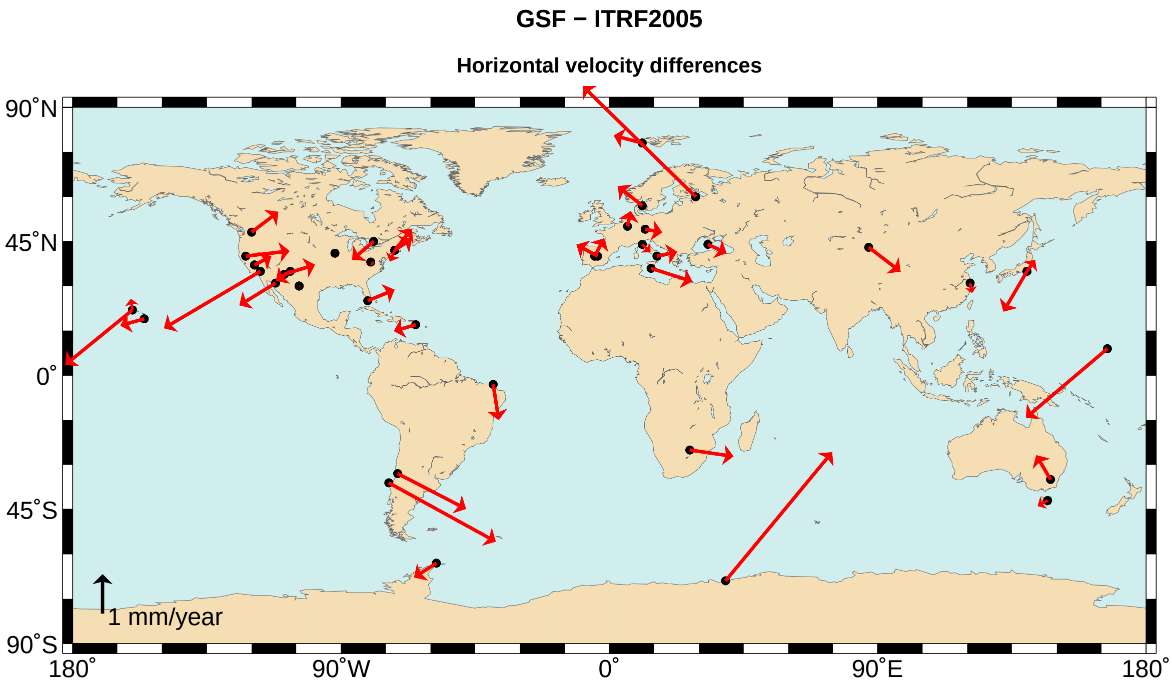

Figure 32: Velocity differences gsf008a−ITRF2005

components as well as of the velocities confirm the overall accuracy of the gsf008a solution at the level of 3.5 mm.

10.3 Celestial Reference Frame at 24, 32, and 43 GHz (CSJ)

A third method of external validation of the ICRF2 is comparing it to celestial frames at other frequencies.

The original ICRF [Ma et al., 1998], its extensions [Fey et al., 2004] and now the ICRF2 are based on VLBI measurements over the last several decades at radio frequencies of 2.3/8.4 GHz. The deep atmospheric window at these radio frequencies combined with the Gigahertz-peaked spectrum nature of many extra-galactic objects facilitates the use of these frequencies for VLBI reference frame work. Historically, the use of these frequencies for radio astronomy at existing antennas contributed to their adoption for use in radio astrometry.

In 1997, as part of the IAU adoption of the original ICRF, resolution B2-d [IAU General Assembly XXIII, 1997] was issued encouraging the extension of the ICRF to other frequencies. In response, VLBI global astrometric measurements have now been made at 24, 32, and 43 GHz and thus can provide the independent checks on the ICRF2 source positions that we desire.

10.3.1 High Frequency Data

With that in mind, we now take a closer look at the high frequency data sets.

- At 24 GHz (K-band), 82 000 observations [Lanyi et al., 2008] have produced a frame of 275 sources covering down to about −40° declination.
- At 8.4/32 GHz (X/Ka-band), 9 400 observations (e.g., Jacobs & Sovers [2008]) have produced a frame of 339 sources covering down to −45°.

- At 43 GHz (Q-band), 19 000 observations [Lanyi et al., 2008] have produced a frame of 132 sources covering down to roughly $-30°$.

All three of these data sets are much, much smaller than the ICRF2's S/X-band data set. Also all three of these data sets cover only part of the southern hemisphere.

10.3.2 Statistical Agreement

We now examine the agreement of the source positions produced at 24, 32, and 43 GHz with our 2.3/8.4 GHz based ICRF2. Table 15 presents the statistics of the comparison with the three high frequency frames and the ICRF2. N_{src} is the number of overlapping sources considered. After removing a three dimensional rotation, the wrms and mean offset were calculated. The results are tabulated in units of μas.

Table 15: Agreement between ICRF2 and frames at 24, 32, and 43 GHz

Frame	N_{src}	$\alpha\cos(\delta)$		δ	
		wrms	offset	wrms	offset
24 GHz	257	115	-2	216	109
32 GHz	320	186	16	261	-8
43 GHz	125	356	20	451	105

For all three frequencies the R.A. agreement is better than the declination agreement. For 24 and 43 GHz, this is because of the limited north-south coverage, i.e., the lack of southern stations in the VLBA network, which creates both a geometrical weakness and which leads to sources in the south being systematically observed at lower elevations and thus more susceptible to atmospheric modeling errors. In particular, there were no dual-frequency plasma calibrations for either the 24- or 43-GHz data sets. The ionosphere was only partially corrected using nearby lines of sight observed to GPS satellites. Tropospheric mis-modeling also contributes to the errors.

For 32 GHz, the declination coordinate was weaker because the observations collected using the two-baseline Deep Space Network had far fewer observations on the north-south California-Australia baseline than on the east-west California-Spain baseline.

Both 32 and 43 GHz observations were limited by low SNR. In addition, the 32 GHz sessions lacked instrumental phase calibrations. These factors will limit the level of agreement with the ICRF2. Yet, despite these limitations, the agreement is good. Recall that the ICRF1 imposed a 250 μas noise floor on its positions. Both the 8 vs. 24 GHz and 8 vs. 32 GHz position agreements are close to or better than this floor. Moreover, our experience suggests that once the VLBA's 43 GHz system sensitivity is improved by increasing from 128 to 512 Mbps sample rates, this band should also agree to ≤ 250 μas.

The most interesting result of this comparison is the 8 vs. 24 GHz wrms agreement in R.A. ($\alpha\cos\delta$) of 115 μas. Given that there is no reason to expect that source structure is systematically different in the declination coordinate and given that a good portion of the scatter is due to thermal and atmospheric errors, this result sets a tight statistical constraint on the core shift and source structure effects between 8 and 24 GHz of ≤ 100 μas for the overlapping sources. Because sources which are observable at both 8 and 24 GHz are expected to be more compact than the average S/X-band ICRF2 source, the 100 μas figure given above may be optimistically biased due to the selection effect of requiring the sources be detectable at high frequencies. Thus users are encouraged to consider detectability at high frequency as one attribute of the highest quality sources.

In summary, since the publication of the ICRF1 in 1998, radio frame work has been extended to three new frequencies: 24, 32, and 43 GHz. Comparing the S/X-band ICRF2 to these independent high frequency data sets shows agreement at the $100-500$ μas level thus lending further validation to the accuracy of the ICRF2.